

An O2If*/WN6 Star Catch in the Act in a Compact HII region in the Starburst Cluster NGC 3603

A. Roman-Lopes^{1*}

¹*Department of Physics - Universidad de La Serena - Cisternas, 1200 - La Serena - Chile*

ABSTRACT

In this letter we report the discovery of an O2If*/WN6 star probably still partially embedded in its parental cocoon in the star-burst cluster NGC 3603. From the observed size of the associated compact HII region, it was possible to derive a probable dynamic age of no more than 600,000 years. Using the computed visual extinction value $A_V \sim 6.0 \pm 0.2$ magnitudes, an absolute visual magnitude $M_V = -5.7$ mag is obtained, which for the assumed heliocentric distance of 7.6 kpc results in a bolometric luminosity of $8 \times 10^5 L_\odot$. Also from the V magnitude and the V-I color of the new star, and previous models for NGC3603’s massive star population, we estimate its mass for the binary (O2If*/WN6 + O3If) and the single-star case (O2If*/WN6). In the former, we find that the initial mass of each component possibly exceeded $80 M_\odot$ and $40 M_\odot$, while in the latter MTT 58’s initial mass possibly was in excess of $100 M_\odot$.

Key words: Stars: Wolf-Rayet; Infrared: Stars: Individual: WR20aa, WR20c; Galaxy: open clusters and associations: individual: Westerlund 2

1 INTRODUCTION

Very massive stars (initial masses $\sim 100 M_\odot$ or higher) are key actors in the energy balance and chemical evolution of galaxies. Due to their powerful winds and expanding HII regions, they inject large quantity of momentum and energetic ultraviolet (UV) photons into the local interstellar medium (ISM), possibly regulating the star formation rate in its vicinity (Vink et al. 2013). However, one of the most fundamental yet still non-answered question in astrophysics is “how do very massive stars form?”. We already have good knowledge on how the formation and early evolution of low mass ($m_* \leq 8 M_\odot$) stars occurs, but the basic processes leading to the formation of massive stars still remain unknown, probably because they are very rare objects whose birthplaces are generally much more distant from us than the nearby sites of low mass star formation. Also, because high mass stars evolve much faster than low mass stars, they are very short lived objects, being usually deeply embedded into their natal environment throughout their very early evolutionary stages.

The very young massive star studied here was first cataloged as MTT 58 by Melnick, Tapia & Terlevich (1989). It probably belongs to NGC 3603, the closest star-burst like cluster (Goss & Radhakrishnan 1969;

Melnick, Tapia & Terlevich 1989; Stolte et al. 2004; Nürnberger 2004) localized at an heliocentric distance of 7.6 ± 0.4 kpc (Crowther et al. 2010). With dozens of very massive stars in its core, with some of them possibly presenting initial masses exceeding 100 - 150 M_\odot (Crowther et al. 2010), NGC 3603 is one of the best Galactic sites for studies on the formation and evolution of very massive stars in the local universe.

2 NEAR-INFRARED SPECTROSCOPIC OBSERVATIONS AND DATA REDUCTION

MTT 58 was chosen for near infrared (NIR) spectroscopic follow-up observations based on its near- to mid-infrared colors, H α and X-Ray emission characteristics (the details on the criteria and general selection methodology are fully discussed in a forthcoming paper - Roman-Lopes submitted). The NIR spectroscopic observations were performed with the Ohio State Infrared Imager and Spectrometer (OSIRIS) at the Southern Astrophysics Research (SOAR) telescope. The J-, H- and K-band data were acquired in 9th May 2011 with the night presenting good seeing conditions. Besides MTT 58, we also obtained NIR spectra for HD93129A (O2If*), WR20a (O3If*/WN6 + O3If*/WN6) and WR42e (O2If*/WN6) (Crowther & Walborn 2011; Roman-Lopes 2012). In Table 1 it is shown a summary of the NIR observations used in this work.

* E-mail: roman@dfuls.cl

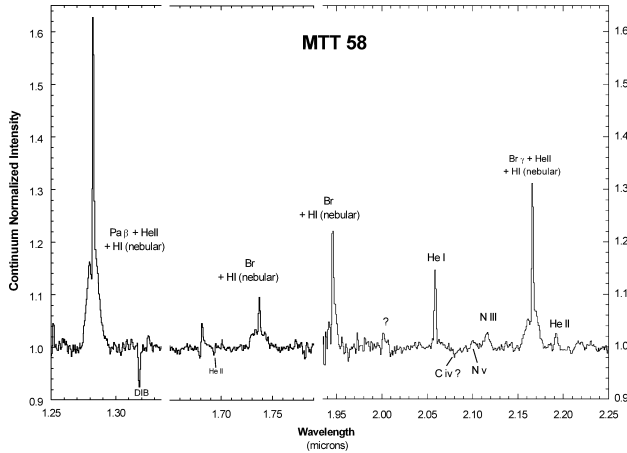


Figure 1. The J- H- and K-band continuum normalized SOAR-OSIRIS spectra of MTT 58, with the main H, He and N emission lines identified by labels. Notice the intense nebular hydrogen recombination lines superimposing the broad emission lines produced by the powerful wind of the embedded star.

Table 1. Summary of the SOAR/OSIRIS dataset used in this work.

Date	09/05/2011
Telescope	SOAR
Instrument	OSIRIS
Mode	XD
Camera	f/3
Slit	1" x 27"
Resolution	1000
Coverage (μm)	1.25-2.35
Seeing (")	1-1.5

The raw frames were reduced following standard NIR reduction procedures. The two-dimensional frames were subtracted for each pair of images taken at the two shifted positions. Next the resultant images were divided by a master normalized flat, and for each processed frame, the J-, H- and K-band spectra were extracted using the IRAF task APALL, with subsequent wavelength calibration being performed using the IRAF tasks IDENTIFY/DISPCOR applied to a set of OH sky line spectra (each with about 30-35 sky lines in the range 12400\AA - 23000\AA). The typical error ($1-\sigma$) for this calibration process is estimated as $\sim 12\text{\AA}$ which corresponds to half of the mean FWHM of the OH lines in the mentioned spectral range. Telluric atmospheric corrections were done using J-, H- and K-band spectra of A type stars obtained before and after the target observations. The photospheric absorption lines present in the high signal-to-noise telluric spectra, were subtracted from a careful fitting (through the use of Voigt and Lorentz profiles) to the hydrogen absorption lines and respective adjacent continuum. Finally, the individual J-, H- and K-band spectra were combined by the average (using the IRAF task SCOMBINE) with the mean signal-to noise ratio of the resulting spectra well above 100.

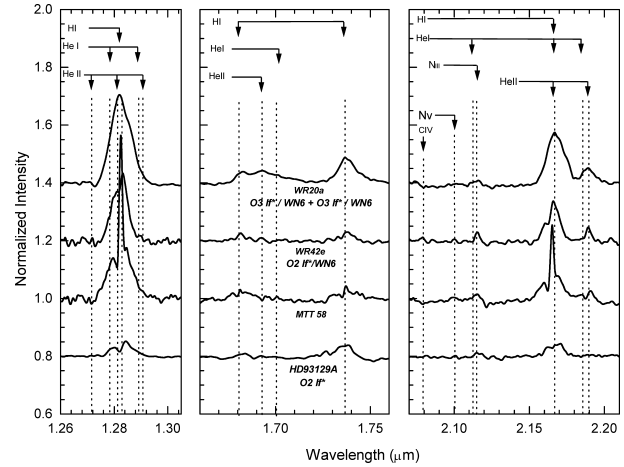


Figure 2. The J- H- and K-band continuum normalized SOAR-OSIRIS spectra of the MTT 58, together with the NIR spectrograms of HD93129A (O2If*), WR42e (O2If*/WN6) and WR20a (O3If*/WN6 + O3If*/WN6), with the main H, He and N emission lines identified by labels. Notice the strong nebular hydrogen recombination narrow lines superimposing the broad emission lines produced by the powerful wind of the embedded star. Besides the nebular emission components, the MTT 58's J-, H- and K-band spectra resemble well those of WR42e.

3 RESULTS

Coordinates and photometry of MTT 58 are shown in Table 2. The B-, V- and I-band magnitudes were taken from the work of Sung & Bessell (2004), while the NIR values were obtained from the Two-Micron All Sky Survey (Cutri et al. 2003), with the absorption-corrected 0.5-10keV Chandra X-ray flux taken from the work of Romano et al. (2008).

3.1 The OSIRIS NIR spectra of MTT 58: An O2If*/WN6 star embedded in a compact HII region

Figure 1 shows the telluric corrected (continuum normalized) J-, H- and K-band SOAR-OSIRIS spectra of MTT 58. They present (despite of the previous subtraction of the background extended nebular components) strong residual hydrogen recombination features that are particularly prominent in the Pa β and Br γ transition lines. They appear as very narrow lines superimposing the broad emission lines generated by the strong stellar wind of the embedded star. The presence of strong narrow nebular line emission indicates that the star is probably immersed in an ionized region.

Figure 2 shows the MTT 58's J-, H- and K-band SOAR-OSIRIS spectra, together with those for HD93129A (O2If*), WR42e (O2If*/WN6) and WR20a (O3If*/WN6 + O3If*/WN6). The MTT 58's J-, H- and K-band spectra resembles well (besides the nebular emission line components) those of WR42e, indicating that the star is a new exemplar of the O2If*/WN6 type. Such objects are rare members of the WNH group that is probably compound by the most massive hydrogen core-burning stars known, which due to their high intrinsic luminosities (close to the Eddington limit), possess emission-line spectra that mimic the spectral appearance of classical WR stars, even in the beginning of their life times

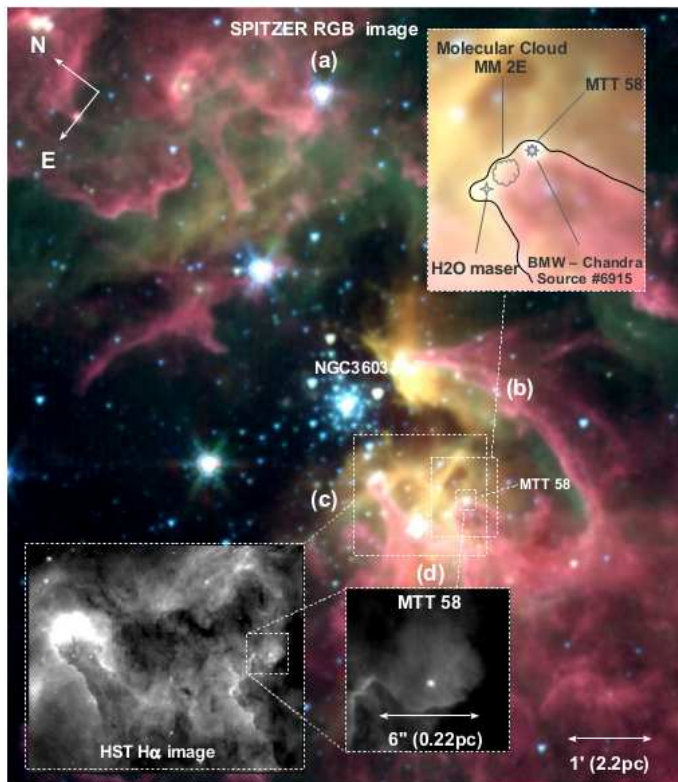


Figure 3. (a) The Spitzer false-color RGB image of the region centered on the core of the NGC3603 star-burst cluster. (b) Zooming of the region in the direction of MTT 58, with the associated pillar (delineated by the black line) mostly visible in the red channel. There we also can see the positions of the BMW - Chandra source #6915 (Romano et al. 2008), the molecular cloud MM 2E (Nürnberg et al. 2002) and the H₂O maser found by Caswell (2004). (c) The HST H α image of NGC 3603 where we can see the spectacular pillars to the south of the cluster core). (d) Detailed view of the H α emission in the vicinity of MTT 58, where we can see the H α counterpart of part of the compact HII region detected by the ATCA observations.

Table 2. Coordinates (J2000), Optical/NIR photometry, and X-ray parameters of the newly-identified O2If*/WN6 star. The BVI photometry was taken from Sung & Bessell (2004), while the near-infrared magnitudes are from Cutri et al. (2003). Finally, the absorption-corrected 0.5-10keV flux is from the work of Romano et al. (2008).

RA=11h15m07.60s	Dec=-61d16m54.8s
B = 16.14	V = 14.76
I = 12.39	J = 10.47±0.02
H = 9.68±0.02	K _S = 9.24±0.02
X-Ray (0.5-10 keV) = $4.23 \times 10^{-17} \text{Wm}^{-2}$	

(Smith & Conti 2008). As a last comment on the MTT 58's spectra, it is interesting to notice that there are two identified lines that appears in absorption. The first is a line at $1.693\mu\text{m}$, that could be due to HeII, while the other is the C IV line at $\sim 2.080\mu\text{m}$. Such absorption lines could be indicative of the presence of an early-O star companion. Indeed, the presence of an X-ray source gives support for this idea.

Figure 3(a) shows a false color RGB image made from the $3.6\mu\text{m}$ (blue), $4.5\mu\text{m}$ (green) and $5.8\mu\text{m}$ (red) Spitzer IRAC images of the region centered in the core of the NGC

3603. The bulk of the remnant of the NGC 3603's parental molecular gas cloud is clearly seen to the south and southwest, where the large-scale star formation is still taking place (de Pree, Nysewander & Goss 1999; McKee & Tan 2002; Nürnberg & Stanke 2003; Nürnberg 2004). As we can see from the figure, MTT 58 is placed at about 1.8 arcmin to the south of the NGC 3603's centre, at the tip of a giant pillar of gas and dust. Figure 3(b) presents a detailed view of the region around MTT 58. There we indicate (besides the star) the position of the X-Ray BMW-Chandra point source #6915 (Romano et al. 2008), and that for the molec-

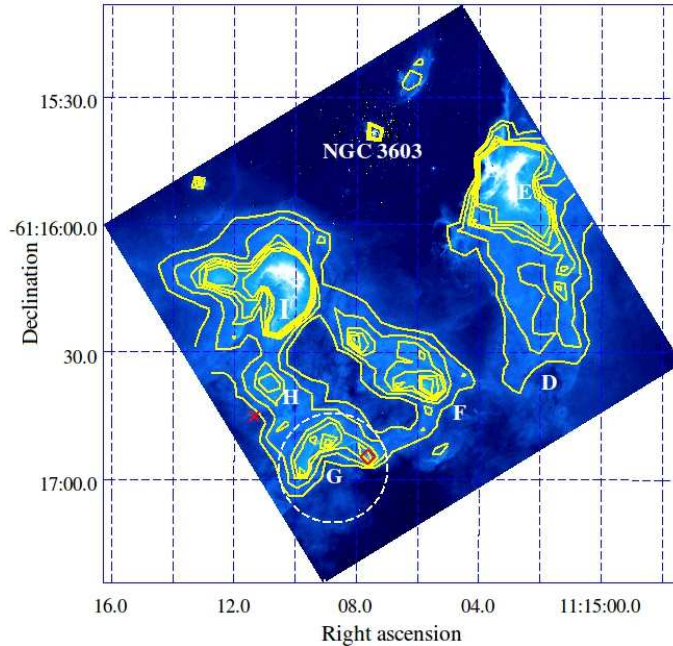


Figure 4. The continuum subtracted HST $H\alpha$ image (logarithmic scale) of the region to the south of NGC 3603 cluster. For the sake of clarity, we also present the $H\alpha$ intensity contours (yellow lines) in steps of 4500, 5500, 6500, 7500 and 8500 units (arbitrary scale). There we indicate the location of the NGC 3603’s cluster and the position of the compact HII regions D, E, F, G, H and I detected by de Pree, Nysewander & Goss (1999) with the Australia Telescope Compact Array (ATCA). The estimate angular size of the compact HII region G, is indicated by the white dashed circle. Also, the location of the O2If*/WN6 star is indicated by the red diamond. Notice the extended emission in the vicinity of MTT 58.

ular cloud MM 2E (Nürnberger et al. 2002) and the H_2O maser found by Caswell (2004). They appear very close in projection (0.15 pc and 0.33 pc, respectively) to MTT 58, with the X-ray source coordinates coinciding exactly with the position of the star. The proximity to a non-destroyed molecular cloud and H_2O maser source, suggest that MTT 58 had no time to completely dissipate its parental molecular cocoon, indicating that it is probably an extremely young O2If*/WN6 star.

3.2 Size and age of the MTT 58’s HII region

As mentioned in the previous section, MTT 58 is possibly powering a compact HII region. We searched in the literature for high spatial resolution radio continuum observations that could give us constraints on the size of the MTT 58’s HII region, and found that de Pree, Nysewander & Goss (1999) observed the region towards MTT 58 with the Australia Telescope Compact Array (ATCA), in the continuum (at 8.8 GHz) and the $H90\alpha$, $He90\alpha$, $C90\alpha$ and $H113\beta$ recombination lines (all with rest frequencies around 8.9 GHz), with angular resolution of $7''$. Their source G with angular size of $26''$ and integrated flux density $S_{tot}=4.4\pm 0.3$ Jy, is one of the strongest sources in the entire region. It has coordinates $\alpha=11:15:08.76$ and $\delta=-61:16:55.7$ (J2000) that matches (considering the associated uncertainties) those of MTT 58. Taking into account the limited ($7''$) ATCA’s spatial resolution, we may consider $26''$ as an *upper limit* for the angular size of the MTT 58’s compact HII region.

We also searched in the Hubble Legacy Archive¹ looking for $H\alpha$ images of NGC 3603, founding that the region towards MTT 58 was observed in the framework of the proposal ID #11360 (P.I. O’Connell, R. W.). Figure 3(c) shows the HST $H\alpha$ image of the southeast part of the NGC 3603’s region, where we can see the bright $H\alpha$ extended emission generated in the top of a spectacular pillar visible to the north of MTT 58. Figure 3(d) presents a detailed view of the $H\alpha$ emission in the vicinity of MTT 58. By scaling the F658N ([NII] 6583) image to the F656N ($H\alpha$ 6552) one (using a set of non-saturated stars), and subtracting the former from the last we obtained a continuum subtracted HST $H\alpha$ image of the region to the south of NGC 3603 cluster. The resulting image is shown in Figure 4 with the location of the NGC 3603 cluster, MTT 58 and the ATCA compact HII regions D, E, F, G, H and I (de Pree, Nysewander & Goss 1999) indicated by labels. As a complement and in order to compare the $H\alpha$ subtracted image with the positions of the 8.8 GHz compact continuum sources detected by de Pree, Nysewander & Goss (1999), we also present the $H\alpha$ intensity contours (represented by the yellow continuum lines), which correspond to 4500, 5500, 6500, 7500 and 8500 counts (arbitrary scale). The $H\alpha$ contours associated to the ATCA source G, present an arc shaped structure (not spherical like in the radio continuum map of de Pree, Nysewander & Goss (1999), probably due to the presence of very dense foreground molecular material well seen (against the bright background extended emission) in Figure 3(b).

¹ <http://hla.stsci.edu/hlaview.html>

We can now estimate the age of the embedded star from the HII region's size, assuming that it reached its initial Strömgren radius in a very short time (a few 10^4 yrs), corresponding to a rapid expansion phase dominated by an R-type shock (Spitzer 1978), and that after this phase it has been expanding in a uniform medium owing to the pressure difference between the hot ionized gas and the outer cool molecular gas. This corresponds to a condition where the HII region expansion is governed by a weak D-type ionization front, with a *rate of expansion* that can be estimated using the equation (Spitzer 1978):

$$R_f(t) = R_i \left(1 + \frac{7CII}{4R_i}t\right)^{\frac{4}{7}}$$

where R_i and R_f are the initial and final values for the Strömgren radius, and CII is the sound speed in the HII region (typically varying from 0.4 to 10 km/s (Israel 1978; Pedlar 1980; Zhu et al. 2005; Mac Low et al 2007; Gendelev & Krumholz 2012; Minier 2013)). In order to be conservative, in the calculation we will assume a mean sound speed of 4 km s⁻¹ and that the numerical density in the beginning of the ultra-compact phase was about 10^5 cm⁻³ (Churchwell 2002), and that the number of Lyman continuum photons (N_{Ly}) emitted by second by an O2If*/WN6 star right in the very beginning of its life-time is about 10^{49} s⁻¹. This can be considered a lower limit because the earliest O super-giant stars are believed to emit much more than 10^{49} s⁻¹ Lyman continuum photons during its main sequence life-time (Smith, Norris & Crowther 2002).

From the angular size of the source G obtained by de Pree, Nysewander & Goss (1999), we can estimate its corresponding dynamical age. The Strömgren radius (Strömgren 1939) for an initial numerical density of 10^5 cm⁻³ and $N_{Ly}=10^{49}$ s⁻¹ is $R_i \sim 0.025$ pc. The upper limit for the final radius R_f can be computed from the angular size ($26''$) estimated from the ATCA observations. Assuming a distance of 7.6 kpc, the corresponding value is $R_f = 0.48$ pc, which applied in Equation 1 results in a dynamical age of $\sim 580,000$ years. On the other hand, in the case in which MTT 58's $N_{Ly}=10^{50}$ s⁻¹ (Crowther & Walborn 2011), the dynamical age would drop by a factor ~ 3.8 , resulting in a much lower age of 150,000 yrs! In any scenario, we conclude that MTT 58 is possibly the youngest Galactic O2If*/WN6 star found to date.

Recently, Roman-Lopes (2012) reported the discovery of an O2If*/WN6 star (WR42e) that is thought to have been ejected from the NGC 3603 cluster core. In this sense we may argue that in the MTT 58's case the situation is probably different. Indeed, considering that an O2If*/WN6 star produces much more Lyman continuum photons than the template (O7v star with $Q_0 \sim 10^{49}$ s⁻¹) we used in our previous calculations, in this case the tremendous ionization front of the O2If*/WN6 star could propagate much quicker than the associated star travel velocity, destroying and dissociating any molecular cloud in its way much earlier of its arrive there. On the other hand, another argument favoring the idea that we are probably looking at an in-situ formation case, is the fact that the observed morphology of the compact HII region studied by de Pree, Nysewander & Goss (1999) is not cometary, like the expected when the ionizing source is traveling with a relatively high transverse velocity (Churchwell 2002).

3.3 Estimating the luminosity of MTT 58

In order to compute estimates for the luminosity and mass of MTT 58, we need to evaluate its visual extinction taking into account that the interstellar reddening law for NGC 3603 is probably abnormal (Pandy, Ogura & Sekiguchi 2000; Sung & Bessell 2004), with a ratio of total to selective extinction value $R_V=3.55\pm 0.12$ (Sung & Bessell 2004). From Table 2, we can see that MTT 58 presents (B-V) color ~ 1.4 mag, which for an assumed mean intrinsic (B-V)₀ value of -0.3 mag (typical for the hottest early-type stars), corresponds to a color excess $E(B-V) \sim 1.7$ mag ($A_V \sim 6.0\pm 0.2$ mag), a extinction value higher than that derived by Sung & Bessell (2004) for the NGC 3603 early-type members ($E(B-V)=1.25$, $A_V=4.4\pm 0.1$), but still compatible with what is expected for an early-type member of NGC 3603 (Sung & Bessell 2004). Assuming that the additional amount of reddening $A_V=1.6$ is generated by the gas and dust present in the compact HII region (e.g. local), we can speculate that the embedded star could be close to disrupt the border of the cavity that is facing the MTT 58's line of sight.

From the computed color excess, one can estimate the MTT 58's absolute magnitude using the distance modulus equation, assuming that the star is placed at an heliocentric distance of 7.6 ± 0.4 kpc (Crowther et al. 2010). We computed $M_V=-5.7$ mag (or $M_K=-5.9$ considering $A_{K_s}=0.12A_V$ - Crowther et al. (2010), which are values that are a bit lower than those obtained by other researchers for stars of similar type (Crowther et al. 2010; Roman-Lopes, Barbá & Morrell 2011; Crowther & Walborn 2011)). However, it is also known that massive stars at their very beginning stages are expected to be less luminous than similar stars at the more evolved main-sequence phase. Considering the derived absolute visual magnitude and assuming a mean bolometric correction $BC \sim -4.3$ mag (Crowther et al. 2010; Crowther & Walborn 2011), we estimate the bolometric magnitude of MTT 58 as $M_{Bol} \sim -10.0$, which corresponds to a total stellar luminosity above $8 \times 10^5 L_{\odot}$.

3.4 Binarity

In Section 3.1 it was mentioned that the H-band MTT 58's spectrum shows the HeII line at $1.693\mu\text{m}$ in absorption, which could indicate the presence of an early-O star companion. As MTT 58 has an associated X-ray source, it is useful to compare its bolometric and X-ray luminosities. From its absorption-corrected 0.5-10keV flux (Table 2), and using the adopted heliocentric distance of 7.6 ± 0.4 kpc (Crowther et al. 2010) we compute an X-ray luminosity $L_X \sim 2.9 \times 10^{32}$ erg s⁻¹ that compared with the bolometric luminosity derived in Section 3.3 results in $L_X/L_{Bol} \sim 10^{-6}$. This result is about ten times greater than the canonical value expected for single stars, e.g. $L_X/L_{Bol} \sim 10^{-7}$ (Chlebowski et al. 1989), favoring the idea that the O2If*/WN6 star probably has an early-O star companion.

If we assume that MTT 58 is a binary star, and from an inspection of their NIR combined spectra (Figure 1), in principle we may conclude that the absence of any HeI line in absorption (e.g. at $1.701\mu\text{m}$ or at $2.113\mu\text{m}$) indicates that the companion of the O2If*/WN6 star should be of spectral

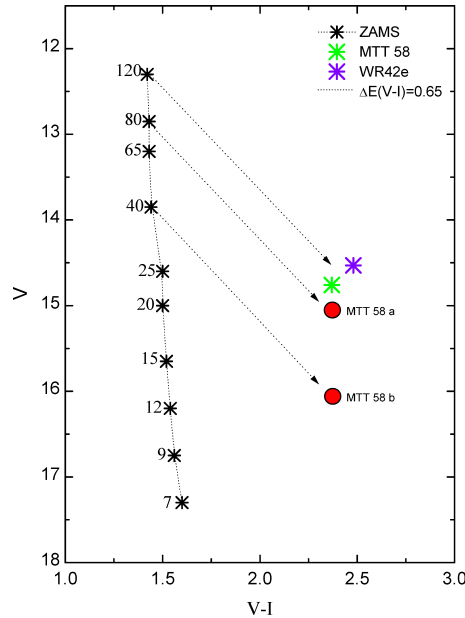


Figure 5. The $V \times (V-I)$ diagram (based on Figure 7 of the work of Sung & Bessell (2004), with MTT 58 represented by the green star (single star case) and red dots (**binary** system case), and WR42e $\sim 130M_{\odot}$ - (Gvaramadze et al. 2013) by the violet star. The non-reddened main sequence at the quoted distance of 7.6 kpc (Crowther et al. 2010) for masses between $7M_{\odot}$ to $120M_{\odot}$ is represented by the black dotted line, with the black stars indicating the position of each mass bin. Also, the reddening vector taken from the work of Sung & Bessell (2004) is represented by the line-dotted arrows. From this diagram we can see that the initial mass of the new O2If*/WN6 star (in the single star case) possibly exceed $100M_{\odot}$. On the other hand, if MTT 58 is assumed to be a binary system compound by a O2If*/WN6 + O3If* system, the individual masses should exceed $80M_{\odot}$ and $40M_{\odot}$, respectively.

type earlier than O4 (Hanson et al. 2005). Indeed, from their NIR spectra of O and early-B stars, one can see that the H-band spectra of O3 stars (like HD 64568 (O3 V) and Cyg OB2 #7 (O3 If*)) present absorption HeII lines at $1.693\mu\text{m}$ that are not as strong as those found in stars later than O4. On the other hand, the 2.189 HeII lines are relatively strong in the K-band spectra of class V stars, becoming more complex in absorption and in emission in the K-band spectrum the O3 If* stars. In this sense, the absence of a strong signature (e.g. in absorption) of the HeII line at 2.189 in the MTT 58's K-band spectrum, enable us (in principle) to rule out a class V type companion star. As mentioned in Section 3.1 the MTT 58's K-band spectrum shows an absorption line at ~ 2.080 microns, which from the associated wavelength we had tentatively identified as due to a CIV line. Interestingly, the K-band spectrum of the O3If* Cyg OB2 #7 does show (Hanson et al. 2005) such an absorption line!

We searched in the HST archive looking for high quality images of the region towards MTT 58 (besides the H α image presented in Figure 3). From a careful inspection of the point spread function of MTT 58 in the HST archive images, we did not find any evidence of a companion, indicating that if MTT 58 is a binary, it is probably formed by a very close system. On the other hand, another possible explanation is that the brightness difference between the two stars is too large (by several magnitudes). In this case, it would be very difficult (if not impossible) to properly separate the brightness distribution of the secondary from that of the main component. However, if the secondary star is assumed to be an O3If* (as the spectral information suggests), the difference in brightness for an O2If*/WN6 star should not be that high. Indeed, from the work of Crowther & Walborn

(2011) one finds that the brightness difference (in terms of bolometric magnitudes) for such kind of stars is possibly not greater than $\sim 1-1.5$ magnitudes. Further NIR and optical spectrophotometric monitoring are certainly necessary to obtain more clues for our assumption of an O2If*/WN6 + O3If* binary system. In this sense, our group in La Serena is planning a long term spectrophotometric monitoring study of this system.

3.5 Mass

We can estimate the mass of MTT 58 by comparing its observed V magnitude and V-I color with those of other NGC 3603 cluster members, presented in Figure 7 of the work of Sung & Bessell (2004). We do that taking into account both, the scenario where it is assumed to be a binary system, as well as that where it is considered as a single star. Also in order to be conservative, we assume that the difference in magnitudes between two stars of O3If* and O2If*/WN6 types is about 1 magnitude (Crowther & Walborn 2011), and to simplify the process we assume that both stars have approximately the same bolometric corrections (a reasonable assumption considering their probable very early spectral types).

Figure 5 shows an adapted version of the $V \times (V-I)$ diagram for NGC 3603 (Sung & Bessell 2004), with MTT 58 (single and binary cases) and WR42e (estimated mass of $\sim 130M_{\odot}$ - Roman-Lopes (2012); Gvaramadze et al. (2013) represented by a green star (single star case) and red dots (binary system case) and violet star, respectively. We added WR42e in the mentioned diagram for comparison purpose because it is of the same spectral type of MTT 58

and probably belongs to the same complex. From this diagram we can see that for the scenario where MTT 58 is considered to be a binary system, the masses of each component would be about $80 M_{\odot}$ (for MTT 58a) and $40 M_{\odot}$ (for MTT 58b). This numbers can be considered reasonable if compared with those from two known very massive binary systems (with similar spectral type and morphology) WR20a (O3If*/WN6 + O3If*/WN6), with masses of 83 and $82 M_{\odot}$ (Bonanos et al. 2004; Smith & Conti 2008), and WR21a (O3If*/WN6 + early-O), for which (Niemela et al. 2008) estimated minimum masses of 87 and $53 M_{\odot}$, respectively. Finally, in the case in which MTT 58 is assumed to be a single star, its initial mass could exceed $100 M_{\odot}$.

4 SUMMARY

In this work we report the discovery of an O2If*/WN6 star probably still embedded in its parental cocoon in the starburst cluster NGC 3603. The new O2If*/WN6 star was previously cataloged as MTT 58 by Sung & Bessell (2004), being apparently placed at the tip of a giant pillar of gas and dust at about 1.8 arcmin (~ 4 pc for the quoted distance of 7.6 kpc - (Crowther et al. 2010) to the south of the NGC 3603's cluster center. The proximity to a non-destroyed molecular cloud, suggests that MTT 58 yet had no time to completely dissipate its parental molecular cocoon, indicating that it is probably an extremely young O2If*/WN6 star.

Another interesting result is that the new O2If*/WN6 star may be the main component of a binary system. Indeed, the presence of a BMW-Chandra X-ray point source coincident with the MTT 58's coordinates and the fact that its NIR spectra present two absorption lines (the HeII $1.693\mu\text{m}$ and the $2.080\mu\text{m}$ CIV lines) possibly generated by an O3If* companion, give strong support for this idea.

From the observed size of the associate compact HII region detected at 3.4 cm by de Pree, Nysewander & Goss (1999) using the Australian Telescope Compact Array (ATCA), it was possible to derive a probable dynamic age of no more than 600,000 years. From the computed visual extinction value $A_V \sim 6.0 \pm 0.2$ mag an absolute visual magnitude $M_V = -5.7$ mag is obtained, which for the assumed heliocentric distance of 7.6 kpc results in a bolometric luminosity of $8 \times 10^5 L_{\odot}$.

Finally, from the V magnitude and V-I colour of the new O2If*/WN6 star and the Figure 7 of the work of Sung & Bessell (2004), we estimate the MTT 58's mass considering the cases in which it is assumed to be a binary system (O2If*/WN6 + O3If stars), and the one in which it is thought to be a single O2If*/WN6 star. In the first case we found that the initial masses of MTT 58a and MTT 58b should be above $80 M_{\odot}$ and $40 M_{\odot}$ respectively. On the other hand, in the scenario were MTT 58 is assumed to be a single star, its initial mass possibly exceeded $100 M_{\odot}$.

ACKNOWLEDGMENTS

This research has made use of the NASA/ IPAC Infrared Science Archive, which is operated by the Jet Propulsion

Laboratory, California Institute of Technology, under contract with the National Aeronautics and Space Administration. This publication makes use of data products from the Two Micron All Sky Survey, which is a joint project of the University of Massachusetts and the Infrared Processing and Analysis Center/California Institute of Technology, funded by the National Aeronautics and Space Administration and the National Science Foundation. Based on observations obtained at the Southern Astrophysical Research (SOAR) telescope, which is a joint project of the Ministério da Ciência, Tecnologia, e Inovação (MCTI) da República Federativa do Brasil, the U.S. National Optical Astronomy Observatory (NOAO), the University of North Carolina at Chapel Hill (UNC), and Michigan State University (MSU). Also, this research has made use of the SIMBAD database, operated at CDS, Strasbourg, France. This work was partially supported by the Department of Physics of the Universidad de La Serena. ARL thanks financial support from Diretoria de Investigación - Universidad de La Serena through Project "Convenio de desempeño DIULS CDI12".

REFERENCES

- Bonanos, A. Z., Stanek, K. Z., Udalski, A., Wyrzykowski, L., ebru, K., Kubiak, M., Szymaski, M. K., Szweczyk, O., Pietrzycki, G., Soszynski, I. 2004, ApJ, 611L, 33B
 Caswell, J. L. 2004, MNRAS, 351, 279
 Chlebowski, T., Harnden, F. R., Jr., Sciortino, S. 1989, ApJ, 341, 427
 Churchwell E. 2002, ARA&A, 40, 27
 Crowther, P. A., Schnurr, O., Hirschi, R., Yusof, N., Parker, R. J., Goodwin, S. P., Kassim, H. A. 2010, MNRAS, 408, 731
 Crowther, P. A. & Walborn, N. R. 2011, MNRAS, 416, 1311
 Cutri, R. M., Skrutskie, M. F., van Dyk, S., Beichman, C. A., Carpenter, and 20 more authors 2003, "The IRSA 2MASS All-Sky Point Source Catalog, NASA/IPAC Infrared Science Archive. <http://irsa.ipac.caltech.edu/applications/Gator/>"
 de Pree, C. G., Nysewander, M. C., Goss, W. M. 1999, AJ, 117, 2902
 Gendele, Leo; Krumholz, Mark R.
 Goss, W. M., Radhakrishnan, V. 1969, ApL, 4, 199
 Gvaramadze, V. V., Kniazev, A. Y., Chen, A.-N.; Schnurr, O. 2013, MNRAS, 430, L20
 Hanson, M. M., Kudritzki, R.-P., Kenworthy, M. A., Puls, J., Tokunaga, A. T. 2005, ApJS, 161, 154
 Israel, F. P. 1978, A&A, 70, 769
 Mac Low, Mordecai-Mark, Toraskar, Jayashree, Oishi, Jeffrey S., Abel, Tom 2007, ApJ, 668, 980
 C. F., McKee J. C., Tan 2002, Nature, 416, 59
 Melnick, J., Tapia, M., Terlevich, R. 1989, A&A, 213, 89
 Minier, V., Tremblin, P., Hill, T., Motte, F., Andr, Ph., and 16 co-authors 2013, A&A, 550, 50
 Niemela V. S., Gamen R. C., Barbá R. H., Fernández Lajús E., Benaglia P., Solivella G. R., Reig P., Coe M. J., 2008, MNRAS, 389, 1447
 Nürnbergger, D. E. A., Bronfman, L., Yourke, H. W., Zinnecker, H. 2002, A&A, 394, 253
 Nürnbergger, D. E. A., Stanke, T. 2003, A&A, 400, 223

- Nürnberg, D. E. A. 2004, ASPC, 322, 75
Pandy, A. K., Ogura, K., & Sekiguchi, K. 2000, PASJ, 52, 847
Pedlar, A. 1980, MNRAS, 192, 179
Roman-Lopes, A., Barba, R. H. & Morrell, N. I. 2011, MNRAS, 416, 501
Roman-Lopes, A. 2012, MNRAS, 427, 65
Romano, P., Campana, S., Mignani, R. P., Moretti, A., Mottini, M., Panzera, M. R., Tagliaferri, G. 2008, A&A, 488, 1221
Smith, L. J., Norris, R. P. F., Crowther, P. A. 2002, MNRAS, 337, 1309
Smith, N. & Conti, P. S. 2008, ApJ, 679, 1467
Spitzer L., 1978, Physical Processes in the Interstellar Medium. Wiley-Interscience, New York
Stolte, A., Brandner, W., Brandl, B. Zinnecker, H., Grebel, E. K. 2004, AJ, 128, 765
Strömngren, B. 1939, ApJ, 89, 526
Sung, H., Bessell, M. S. 2004, AJ, 127, 1014
Vink, J. S., Heger, A., Krumholz, M. R., Puls, J. and 24 more authors 2013, astro-ph arXiv:1302.2021v2
Zhu, Qing-Feng, Lacy, John H., Jaffe, Daniel T., Richter, Matthew J., Greathouse, Thomas K. 2005, ApJ, 631, 381